Inorganic Chemistry

Article

pubs.acs.org/IC

Mixed Pentele-Chalcogen Cationic Chains from Aluminum and Gallium Halide Melts

Andreas Eich,[†] Thomas Bredow,[‡] and Johannes Beck*[,†]

[†]Institute for Inorganic Chemistry, University of Bonn, Gerhard-Domagk-Strasse 1, 53121 Bonn, Germany

[‡]Mulliken Center for Theoretical Chemistry, Institute for Physical and Theoretical Chemistry, University of Bonn, Beringstrasse 4, 53115 Bonn, Germany

Supporting Information

ABSTRACT: The reactions of tellurium or selenium with bismuth or antimony in chloridogallate and iodidoaluminate melts in the presence of group 15 trihalides as weak oxidants yielded the compounds $(Sb_2Te_2)[GaCl_4]$ (**1**), $(Sb_2Te_2)I[AlI_4]$ (**2**), $(Bi_2Te_2)Cl[GaCl_4]$ (**3a**), $(Bi_2Se_2)Cl[GaCl_4]$ (**3b**), $(Sb_3Te_4)[GaCl_4]$ (**4**), and $(SbTe_4)[Ga_2Cl_7]$ (**5**). In the crystal structures one-dimensional polymeric cations $(Sb_2Te_2^+)_n$ (**1**), $(Sb_2Te_2^{2+})_n$ (**2**), $(Bi_2Te_2^{2+})_n$ (**3a**), $(Bi_2Se_2^{2+})_n$ (**3b**), $(Sb_3Te_4^+)_n$ (**4**), and $(SbTe_4^+)_n$ (**5**) are present. The polymeric cationic strands in **2**, **3a**, **3b**, and **4** consist of pentele/chalcogen dumbbells, which are connected to ladder-shaped bands. The strands in **1** and **5** consist of condensed rings that involve four-membered Sb_2Te_2 rings for **1**, and five-membered $SbTe_4$ rings for **5**. The counteranions are the weakly coordinating $[GaCl_4]^-$, $[AlI_4]^-$, and $[Ga_2Cl_7]^-$ in addition to Cl^- and I^- anions, which are coordinated to the atoms of the cations. The crystal structures of **1**−**4** are characterized by a statistical disorder in the anions with alternatively occupied positions for the Al and Ga atoms. For **4** superstructure reflections appear in the diffractions patterns, indicating a partial order. A correct assignment of the Sb and Te positions in the cation of **5** was achieved by periodic quantum-chemical calculations, which were performed via a Hartree−Fock density functional theory hybrid method. A clear preference of the 4-fold coordinated site was obtained for Sb.

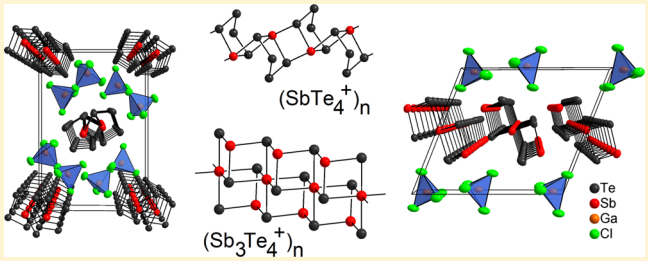

INTRODUCTION

The heavier, electron rich main group elements form polycationic clusters which occur as both unassociated species or polymeric strands. Besides the large number of molecular homoatomic clusters such as $(E_4)^{2+}$ (E = S, Se, Te), $(Te_6)^{2+}$, or $(S_{19})^{2+}$,[1] a series of heteronuclear polycationic clusters composed of elements of group 15 and 16 have been reported: $(As_3Se_4)^+$,[2] $(Bi_4Ch_4)^{4+}$ (Ch = S, Se, Te),[3] $(Sb_7Te_8)^{5+}$,[4] $(Sb_7Se_8)^{5+}$,[5] $(Sb_{10}Se_{10})^{2+}$,[6] $(Sb_7Ch_8X_2)$ (Ch = S, Se; X = Cl, Br),[5,7] or $(Sb_{13}Se_{16}Br_2)^{5+}$. The latter species has a structure consisting of four corner-sharing cubes.[7] As the general structural principle, these polycations form structures consisting of rings, cages, or interconnected cages.

The class of polymeric polycations is also common for various homo- and heteronuclear species with different structural types. For example, $(Te_7^{2+})_n$ exists in two modifications, as a folded band in $Te_7[WOX_4]_2$ (X = Cl, Br) and $Te_7[Be_2Cl_6]$[8] and as strands of connected six-membered rings in $Te_7[AsF_6]_2$.[9] The cationic tellurium strand $(Te_8^{2+})_n$ occurs as two differently folded chains of connected six-membered rings in $Te_8[Bi_4Cl_{14}]$, $Te_8[U_2Br_{10}]$, and $Te_8[NbOCl_4]_2$.[10] A combination of two different polymeric tellurium strands is present in $(Te_4)(Te_{10})[Bi_4Cl_{16}]$.[8a] The structure of $(Te_6^{2+})_n$ is built of strands consisting of unusual five-membered Te_5 rings.[11] Mixed tellurium/selenium polymeric chains built of connected four- and five-membered rings are present in the structures of $(Se_4Te_3)[WOCl_4]_2$ and $(Se_{4.85}Te_{3.15})[WOCl_4]_2$.[12] The general structural motif of these 1D strands of connected chalcogen atoms is connected rings.

The number of known polymeric pentele/chalcogen cations is limited to $(Sb_2Te_2^+)_n$,[13] $(Sb_2Te_2^{2+})_n$, $(Bi_2Te_2^{2+})_n$,[14] $(Bi_2Se_2^{2+})_n$, and $(Bi_4Te_4^{4+})_n$,[15] which show interesting electrical transport properties such as anisotropic or n-type semiconductivity. The structure of the cations $(Sb_2Te_2^+)_n$ consists of connected four-membered rings similar to $(Te_4^{2+})_n$ in $(Te_4)(Te_{10})[Bi_4Cl_{16}]$.[8a] The other known mixed chains establish the structure motif of ladder shaped strands related to those known for the homonuclear tellurium strands in Te_2Br[16] and $(Te_{15}X_4)_n[MOX_4]_{2n}$ (X = Cl, Br; M = Mo, W).[17]

By synthetic work in chloridogallate and iodidoaluminate melts we found the polymeric ladder shaped cations $(Sb_2Te_2^+)_n$ (**1**), $(Sb_2Te_2^{2+})_n$ (**2**), $(Bi_2Te_2^{2+})_n$ (**3a**), and $(Bi_2Se_2^{2+})_n$ (**3b**) as new compounds. Moreover, the unprecedented polymeric cations $(Sb_3Te_4^+)_n$ (**4**) with a "double ladder" structure and $(SbTe_4^+)_n$ (**5**) with a unique structure of connected five-membered rings were isolated.

Received: September 10, 2014
Published: December 30, 2014

DOI: 10.1021/ic502199v
Inorg. Chem. 2015, 54, 484−491

Table 1. Crystallographic Data and Details of the Structure Determinations for $(Sb_2Te_2)[GaCl_4]$ (1), $(Sb_2Te_2)I[AlI_4]$ (2), $(Bi_2Te_2)Cl[GaCl_4]$ (3a),$(Bi_2Se_2)Cl[GaCl_4]$ (3b), $(Sb_3Te_4)[GaCl_4]$ (4), and $(SbTe_4)[Ga_2Cl_7]$ (5)[a]

	1	2	3a	3b	4	5
formula	$Cl_4GaSb_2Te_2$	$AlI_5Sb_2Te_2$	$Bi_2Cl_5GaTe_2$	$Bi_2Cl_5GaSe_2$	$Cl_4GaSb_3Te_4$	$Cl_7Ga_2SbTe_4$
M_r/g mol^{-1}	710.22	1160.18	920.13	822.85	1087.17	1019.74
space group	$P\bar{1}$	$P2_1/n$	$C2/m$	$C2/m$	$C2/m$	$P2_1/n$
a/Å	9.4444(2)	10.2435(6)	12.8796(3)	12.6243(9)	14.451(2)	7.1476(5)
b/Å	13.4186(2)	8.5420(5)	4.2248(1)	4.0495(2)	4.1958(4)	18.854(2)
c/Å	17.9179(3)	17.468(1)	10.5753(3)	10.4926(7)	12.899(1)	12.8699(8)
α/deg	75.372(1)	90	90	90	90	90
β/deg	87.831(1)	97.905(2)	98.535(2)	99.945(4)	111.797(4)	94.240(4)
γ/deg	88.556(1)	90	90	90	90	90
V/Å^3	2195.28(7)	1513.9(2)	569.07(2)	528.34(6)	726.3(1)	1729.7(2)
Z	8	4	2	2	2	4
refins ($I > 2\sigma(I)$)	7648	2452	713	569	703	2486
refined params	325	101	39	39	44	127
$R(F)/wR(F^2)$ ($F_o > 4\sigma(F_o)$)	0.0362/0.0663	0.0428/0.0874	0.0171/0.0396	0.0382/0.0679	0.029/0.0488	0.0507/0.0944

[a]Standard deviations given in brackets refer to the last significant digit.

EXPERIMENTAL SECTION

General Synthetic Procedures and Materials. The details of the synthetic procedures are described in ref 4. All syntheses were performed between 50 and 190 °C in flame-dried, evacuated glass ampules (Simax glass, length approximately 90 mm, outer diameter 14 mm, wall thickness 1.5 mm). Tube furnaces used for syntheses were aligned at an angle of about 30° to the horizontal to keep the melt compacted in the hot zone.

The iodides of sodium, silver, copper(I), aluminum, and antimony were commercial products delivered in sealed ampules, which were opened in the glovebox and used without further treatment.

$(Sb_2Te_2)[GaCl_4]$ (1). Under argon atmosphere, 91.8 mg (0.72 mmol) of tellurium, 58.4 mg (0.48 mmol) of antimony, 54.7 mg (0.24 mmol) of antimony trichloride, 348.6 mg (1.98 mmol) of gallium trichloride, and 10.5 mg (0.18 mmol) of sodium chloride were filled in a glass ampule, which was evacuated to approximately 6×10^{-2} mbar, flame-sealed, and placed in a horizontal tube furnace. After 13 days at 125 °C, silvery shiny rod-shaped crystals were obtained in 30% estimated yield in a black melt.

$(Sb_2Te_2)I[AlI_4]$ (2). A 122.3 mg (0.20 mmol) portion of antimony telluride, 80.4 mg (0.16 mmol) of antimony triiodide, 403.6 mg (0.99 mmol) of aluminum triiodide, and 26.9 mg (0.18 mmol) of sodium iodide were annealed in an evacuated glass ampule at 100 °C for 7 days and at 170 °C for additional 5 days. Compound **2** formed black cube-shaped crystals emerging from an orange melt, which solidified at ambient temperature. During the manual separation, the crystals were revealed to be intergrown agglomerates of silvery shiny thin square plate-shaped crystals.

An increased yield can be achieved by replacing sodium iodide with copper(I) iodide or silver iodide and annealing the ampules stepwise at 100 °C for 7 days, 170 °C for 5 days, and finally at 190 °C for 8 days. Cooling down to room temperature with 6 °C/h yielded **2** at approximately 30%. When using the adjuvant CuI, black block-shaped crystals were formed, and when using AgI, silvery rod-shaped crystals were formed. The identities of both forms were confirmed by lattice constant determinations on isolated single crystals. The crystals from batches of **2** run with the adjuvant AgI are mechanically sensitive and easily fan out on mechanical strain.

$(Bi_2Te_2)Cl[GaCl_4]$ (3a) and $(Bi_2Se_2)Cl[GaCl_4]$ (3b). For the synthesis of **3a**, 76.6 mg (0.6 mmol) of tellurium, 83.6 mg (0.4 mmol) of bismuth, 63.1 mg (0.2 mmol) of bismuth trichloride, and 105.6 mg (0.6 mmol) of gallium trichloride were loaded into a glass ampule, which was sealed under vacuum. For **3b**, tellurium was replaced by the respective molar amount of selenium. The ampules were placed in tube furnaces aligned at an angle of about 30° to the horizontal. For **3a**, the ampule was annealed at 120 °C for 6 days and at 140 °C for an additional 7 days. For **3b**, the ampule was annealed at 50 °C for 11 days and at 100 °C for an additional 9 days. Compound **3a** crystallized in the form of black needles, **3b** as dark red needles. Crystals isolated from the black melt had a pronounced tendency to form intergrown agglomerates. In the synthesis of **3a**, sodium chloride or tetraphenylphosphonium chloride may be added to the reaction mixture as an adjuvant. The use of $[P(C_6H_5)_4]Cl$ is advantageous since a less viscous melt is obtained, which alleviates the separation of the crystals.

By adding sodium chloride to the reaction mixture for the synthesis of **3b**, $(Bi_4Se_4)[GaCl_4]_4$ is obtained in the form of yellow crystals. This compound crystallizes isotypically to the aluminum containing congener $(Bi_4Se_4)[AlCl_4]_4$.[3a]

$(Sb_3Te_4)[GaCl_4]$ (4). A 45.2 mg (0.36 mmol) portion of tellurium, 29.2 mg (0.24 mmol) of antimony, 27.4 mg (0.12 mmol) of antimony trichloride, 174.0 mg (0.99 mmol) of gallium trichloride, and 60.0 mg (0.16 mmol) of tetraphenylphosphonium chloride were filled in a glass ampule, which was evacuated and sealed. On annealing at temperatures between 50 and 140 °C, crystals appeared within 1−3 weeks in the form of silvery, metallic shiny rods in an estimated yield of 15%. Tetraphenylphosphonium chloride may be replaced by sodium chloride. At slightly higher reaction temperatures between 130 and 160 °C, crystallization starts after 3 days. The disadvantage of this variant is the much higher viscosity of the melt, which hampers the manual separation of the crystals.

$(SbTe_4)[Ga_2Cl_7]$ (5). A 45.2 mg (0.36 mmol) portion of tellurium, 29.2 mg (0.24 mmol) of antimony, 27.4 mg (0.12 mmol) of antimony trichloride, 174.0 mg (0.99 mmol) of gallium trichloride, 60.0 mg (0.16 mmol) of tetraphenylphosphonium chloride, and 14.4 mg (0.09 mmol) of tellurium dioxide were placed in a glass ampule, which was flame-sealed under dynamic vacuum. After 60 days at 50 °C, compound **5** was obtained as black needles in an estimated yield of 70% in addition to small residues of unreacted antimony in a colorless melt.

Elemental Analysis by Energy Dispersive Electron-Beam X-ray Fluorescence. Samples of all compounds were examined for their composition via energy dispersive electron-beam X-ray fluorescence. Selected crystals were fixed on a carbon coated sample holder, transferred into the instrument under exclusion of air, sputtered with gold under low pressure using an argon plasma (SPI Module Sputter Coater), and irradiated under high vacuum with 20 kV accelerated electrons (Zeiss DSM 940, detector Genesis 2000, Edax). In all cases, 3−5 crystals of the respective compound were investigated with about five measurement points each. Some of the examined crystals were covered with gallium trichloride or gallate melt adherences on their surface. Due to these residues originating from the synthetic procedures, the obtained values for gallium and chlorine came out too high for **1**. Depending on the actual position of the electron beam on the crystal surface the amount of adherences varied, which led to

DOI: 10.1021/ic502199v
Inorg. Chem. 2015, 54, 484−491

high standard deviations for the composition of **3b**. The complete EDX analyses results for all compounds **1**−**5** are located in Supporting Information Table S2.

Crystal Structure Determinations. All compounds under study are highly moisture sensitive. Crystals were manually selected from the melts, cleaned from adherences in perfluorinated polyether (Fomblin-Y/Sigma-Aldrich or NVH Oil/Jena Bioscience), and transferred from this medium into the cold N_2 stream of the crystal cooling device of a Bruker-Nonius Kappa-CCD diffractometer equipped with graphite monochromatized Mo Kα radiation. The crystals of **2** were measured using a Bruker X8 Kappa ApexII diffractometer. Data collections were performed at −150 °C (123 K). All crystal structures were solved by direct methods and refined based on F^2 with anisotropic displacement parameters for all atoms.[18] A semiempirical absorption correction was applied to all data sets.[19,20] In the cases of compounds **2**, **4**, and **5**, special care was taken for the correct assignment of the heavy atom positions Te/Sb, which were possible on the basis of the diffraction data. All respective positions were initially treated as occupied by tellurium solely and refined with free occupation parameters. Because of the slightly higher scattering factor of tellurium, the atomic positions occupied by antimony are thus falsely assigned and are expected to obtain an occupation factor of less than 1. Actually, significant differences in the occupation factors were found, which allowed for the assignment of the respective atom positions. Table S1 (see Supporting Information) shows the obtained occupation factors and the subsequent Te/Sb site assignments in the structures of $(Sb_2Te_2)I[AlI_4]$ (**2**), $(Sb_3Te_4)[GaCl_4]$ (**4**), and $(SbTe_4)[Ga_2Cl_7]$ (**5**). The analysis of the coordination of the Sb and Te atoms by Cl and I atoms of neighboring anions supports the chosen Sb/Te distribution (Supporting Information Table S5). In the structures of **2**, **3a**, **3b**, and **4**, disorder models for the Al or Ga atoms had to be set up (see below).

Table 1 and Tables S3−S7 (Supporting Information) contain the crystallographic data and details of the structure determinations. Graphical representations were made using the program DIAMOND.[21] Further details of the crystal structure investigations may be obtained from the Fachinformationszentrum Karlsruhe, 76344 Eggenstein-Leopoldshafen, Germany, e-mail crysdata@fiz-karlsruhe.de, by quoting the deposit numbers CSD-428454 for **1**, CSD-428455 for **2**, CSD-428453 for **3a**, CSD-428452 for **3b**, CSD-428456 for **4**, CSD-428457 for **5**.

Quantum-Chemical Calculations. In order to clarify the structure of **5**, periodic quantum-chemical calculations were performed with the crystalline orbital program package CRYSTAL14.[22] The Hartree−Fock density functional theory (HF-DFT) hybrid method PW1PW was employed[23] since it has provided reliable data for the thermodynamic and structural properties of solids before. Atom-centered basis sets of triple-ζ quality were used, ECP28MDF for Sb[24] and Te,[25] where the inner 1s, 2sp, and 3spd shells were replaced with a scalar-relativistic effective core potential, and all-electron 864−111G31d and 86-311G1d basis sets from the CRYSTAL homepage for Ga and Cl, respectively. Integral tolerances were set to high values (9 9 9 9 18), a very fine point grid (XXLGRID) was chosen for numerical integration of the exchange-correlation energy, and an 8 × 8 × 8 Monkhorst−Pack grid was employed for reciprocal space sampling. With these rather accurate settings, full optimizations of all atomic positions of the primitive unit cell were performed with fixed lattice constants set to the values measured in the present study (see Table 1).

RESULTS AND DISCUSSION

Synthesis and Properties. Compounds **1**−**5** were obtained from melts mainly composed of gallium trichloride for **1**, **3a**, **3b**, **4**, and **5**, and aluminum triiodide for **2**. Antimony or bismuth trihalides were used as mild oxidants toward the respective elements. The tentative reaction equations are

$$5Sb + 6Te + SbCl_3 + 3GaCl_3 \rightarrow 3(Sb_2Te_2)[GaCl_4]\ (\mathbf{1}) \quad (1)$$

$$4Sb + 6Te + 2SbI_3 + 3AlI_3 \rightarrow 3(Sb_2Te_2)I[AlI_4]\ (\mathbf{2}) \quad (2)$$

$$4Bi + 6Te + 2BiCl_3 + 3GaCl_3 \rightarrow 3(Bi_2Te_2)Cl[GaCl_4]\ (\mathbf{33}) \quad (3)$$

$$4Bi + 6Se + 2BiCl_3 + 3GaCl_3 \rightarrow 3(Bi_2Se_2)Cl[GaCl_4]\ (\mathbf{3b}) \quad (4)$$

$$8Sb + 12Te + SbCl_3 + 3GaCl_3 \rightarrow 3(Sb_3Te_4)[GaCl_4]\ (\mathbf{4}) \quad (5)$$

$$2Sb + 12Te + SbCl_3 + 6GaCl_3 \rightarrow 3(SbTe_4)[Ga_2Cl_7]\ (\mathbf{5}) \quad (6)$$

The additions of sodium chloride or sodium iodide were essential in the syntheses of **1** and **4**. Without the addition of NaCl, no crystalline products at all were formed in attempted reactions for **4**. Sodium halides dissolve in the reaction melts, forming $Na[GaCl_4]$ and $Na[AlI_4]$ and lowering the Lewis acidity of the melts. The adjuvant sodium halides were not incorporated into the crystals as shown by EDX analyses and remained in the viscous melts. Crystals of all compounds under study are black or shiny metallic, only $(Bi_2Se_2)Cl[GaCl_4]$ (**3b**) forms dark red crystals. Compounds **1** and, particularly, **4** were obtained as intergrown crystal bundles. For the separation of single crystals, mechanical splitting along their long axes had to be applied. Compounds **3a** and **3b** crystallize in extremely thin needles, which are sensitive to cleavage during any mechanical treatment. Crystals of **2** grow in block shaped crystals, but show analogously a high sensitivity to mechanical manipulation. Compounds **1**−**4** crystallize from the melts at estimated yields of 10−30%. All attempts to synthesize a compound of the composition $(Bi_3Te_4)[GaCl_4]$ in an analogous way to the synthesis of $(Sb_3Te_4)[GaCl_4]$ (**4**) were unsuccessful since only $(Bi_2Te_2)Cl[GaCl_4]$ (**3a**) was obtained.

Tellurium dioxide, which dissolves in the acidic reaction melt, was the crucial adjuvant in the synthesis of **5**. Compared to the rather low yields of compounds **1**−**4**, **5** is obtained at high yield of about 70%. No other products besides unreacted antimony and small residues of an almost colorless melt were present in the closed reaction ampules, and no oxygen was detected in the reaction product.

Over the course of our investigations, tetraphenylphosphonium chloride was an invaluable adjuvant. On one hand, $[P(C_6H_5)_4]Cl$ has an improving influence on the products, and on the other hand, it allows for new products. The synthesis of $Ag(Sb_7Te_8)[GaCl_4]_6$ was only possible in the presence of this adjuvant.[5] Mixtures of $[P(C_6H_5)_4]Cl$ and $GaCl_3$ instantaneously liquefy at room temperature by forming $PPh_4[GaCl_4]$ and can be conceived as an ionic liquid. Additionally, $[P(C_6H_5)_4]Cl$ lowers the acidity of the melts by providing Cl^- anions similar to NaCl. During the syntheses of $Na(Sb_7Te_8)[GaCl_4]_6$ and $(Sb_7Se_8Cl_2)[GaCl_4]_3$, the yield, crystal quality, and crystal size could be improved substantially by adding tetraphenylphosphonium chloride to the basic educt mixture.[5] The reason may be attributed to the lower viscosity of the melts and a higher ion mobility.

The dark-red, block-shaped crystals of $Cu[AlI_4]$ were obtained as byproducts in the synthesis of **2** with CuI used as the adjuvant. In all three applied synthetic procedures for **2**, yellow rod-shaped crystals were found, which were identified as

DOI: 10.1021/ic502199v
Inorg. Chem. 2015, 54, 484−491

$(SbI_2)[AlI_4]$.[26] Both compounds can be obtained individually by reacting CuI and SbI_3 with AlI_3 at 190 °C, respectively.

All attempts to measure the electrical conductivity of the selected crystals were hampered by the brittleness and mechanical instability of the crystals of all the compounds (Supporting Information Figures S9 and S10). However, semiconducting behavior is expected, as reported for $(Bi_2Se_2)Cl[AlCl_4]$, $(Bi_4Te_4Br_2)[Al_2Cl_{6-x}Br_x]Cl_2$,[15] and $(Bi_2Te_2)Br[AlCl_4]$.[14]

Crystal Structures of 1, 2, 3a, and 3b: Compounds with a $(Pn_2Ch_2^{1+/2+})_n$ Polymeric Cation. One-dimensional polymeric $(Pn_2Ch_2^{1+/2+})_n$ cations are present in the crystal structures of $(Sb_2Te_2)[GaCl_4]$ (**1**), $(Sb_2Te_2)I[AlI_4]$ (**2**), $(Bi_2Te_2)Cl[GaCl_4]$ (**3a**), and $(Bi_2Se_2)Cl[GaCl_4]$ (**3b**). Compound **1** contains the polymeric cation $(Sb_2Te_2^+)_n$ and is isotypic to the known aluminum containing analogue $(Sb_2Te_2)[AlCl_4]$.[13] The structure consists of discrete $[GaCl_4]^-$ anions and two symmetrically independent polymeric cations, which are composed of approximately parallel arranged four-membered Sb_2Te_2 rings. These rings are connected by Sb–Sb and Sb–Te bonds to infinite chains. Tellurium occupies both the 2-fold and 3-fold coordinated positions, the latter ones carrying the formally positive charges (Supporting Information Figure S1). According to the Zintl rules, any change to the charge of the cation will lead to an altered structure. This rule holds since the structures of **2**, **3a**, and **3b**, containing the polymeric cation $(Pn_2Ch_2^{2+})_n$, exhibit as a consequence of the charge +2 on each Pn_2Ch_2 unit, a different connection between the Pn_2Ch_2 ring units with respect to the structure of **1**. The three compounds crystallize all in space group $C2/m$, but only $(Bi_2Te)Cl[GaCl_4]$ (**3a**) and $(Bi_2Se_2)Cl[GaCl_4]$ (**3b**) are isotypic. All heavy atoms occupy exclusively special positions in the mirror planes, and all pentele and chalcogen atoms are triply coordinated (Figure 1).

Pn–Ch dumbbells are connected to infinite ladder-shaped bands with zigzag conformations, running along the crystallographic *b* direction. In each of the bands of **3a** and **3b**, two different Bi–Ch bonds are present, one along the band and the other across. The bond lengths are uniform in the bismuth-containing compounds **3a** and **3b** (Bi–Te 2.9631(5) and 2.9673(3) Å, Bi–Se 2.781(1) and 2.782(2) Å). In $(Sb_2Te_2)I[AlI_4]$, the Sb–Te bond lengths across the band are 2.805(1) and 2.823(1) Å. In contrast, the bond lengths along the band are significantly longer in the range between 2.918(1) and 3.095(1) Å (Table 2).

The bond angles within the ladder-shaped cations are uniform in all three structures and close to 90° (Supporting Information Tables S6 and S7). The structures of the cations thus resemble the ternary pentele chalcogenide halides SbTeI,[27] BiTeCl,[28] and BiSeCl,[29] from which they are formally derived, by replacing every second halide ion with halogenido aluminates and gallates. The remaining halide ions have different functions. In the structures of **3a** and **3b**, the chloride ions bridge the Bi atoms of the neighboring polymeric chains with Bi–Cl distances of 3.1396(2) Å for **3a** and 3.0875(5) Å for **3b**, giving the two structures a pronounced layered character. The arrangement of $[AlI_4]^-$ and I^- ions in the structure of **2** is different. No bridging halide atoms between adjacent cationic strands are present. Instead, the cationic strands are surrounded all around by $[AlI_4]^-$ anions, retaining the one-dimensional character. The discrete iodine atoms form asymmetric bridges over each of the two Sb atoms with Sb–I bonds of 3.051(1) and 3.199(2) Å.

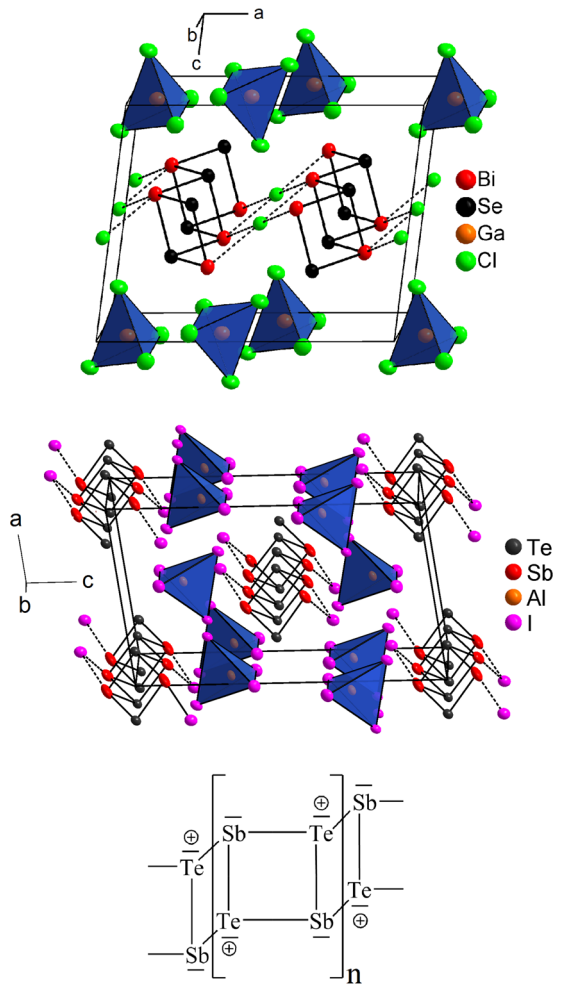

Figure 1. Unit cells of the structures of $(Bi_2Se_2)Cl[GaCl_4]$ (**3b**) (top) and $(Sb_2Te_2)I[AlI_4]$ (**2**) (middle). The $[GaCl_4]^-$ and $[AlI_4]^-$ ions are shown as discrete tetrahedra. The atoms are represented by thermal ellipsoids scaled to include a probability of 90%. Both structures are depicted in an idealized way since only one-half of the disordered Ga and Al atoms is shown. For $(Sb_2Te_2)I[AlI_4]$ only the atom sites Al(1) with 85% occupation are depicted. On bottom a Lewis formula for the $(Sb_2Te_2)^{2+}$ polymeric cation is given. Formulas for $(Bi_2Te_2)^{2+}$ and $(Bi_2Se_2)^{2+}$ are analogous.

Table 2. Bond Lengths/Å in the Crystal Structure of $(Sb_2Te_2)I[AlI_4]$ (2)[a]

bond	length
$Sb1–Te1^{II}$	2.8059(9)
Sb1–Te1	2.962(1)
Sb1–Te2	2.918(1)
$Sb2^{I}–Te1$	3.095(1)
$Sb2^{III}–Te2$	2.8238(9)
Sb2–Te2	2.947(1)

[a]Symmetry operations: I = $x, -1 + y, z$; II = $1 - x, 1 - y, 1 - z$; III = $1 - x, 2 - y, 1 - z$.

Crystal Structure of 4: Hypervalency in the Polymeric Cation $(Sb_3Te_4^+)_n$. The crystal structure of $(Sb_3Te_4)[GaCl_4]$ (**4**) contains a novel polymeric pentele/chalcogen cation. Figure 2 shows the unit cell of **4** and a section of the cationic chain. As a peculiarity, one of the three Sb atoms of the formula entity has a 6-fold coordination in the form of an almost undistorted $SbTe_6$ octahedron. This $SbTe_6$ coordination entity

DOI: 10.1021/ic502199v
Inorg. Chem. 2015, 54, 484–491

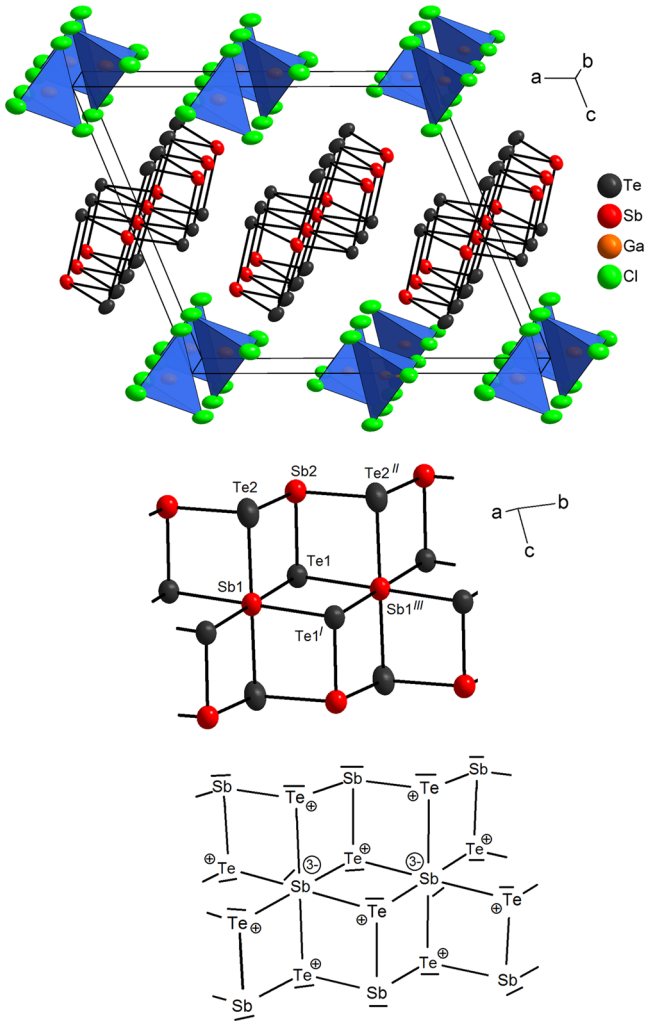

Figure 2. Unit cell of the structure of $(Sb_3Te_4)[GaCl_4]$ (**4**) (top). The $[GaCl_4]^-$ ions are represented as discrete tetrahedra. The atoms are represented by thermal ellipsoids scaled to include a probability of 90%. The structure is idealized, and only one-half of the disordered atoms Ga and Cl(1) is shown. In the middle a detailed view of a section of the cationic chain is given, on the bottom the respective Lewis formula in classical terms, assuming two-center two-electron bonds between all atoms (see text). Selected bond lengths/Å: Sb1–Te1 3.0257(5), Sb1–Te2 3.0280(7), Sb2–Te1 2.8686(9), Sb2–Te2 2.8876(7).

is known from the molecular double-cube shaped $(Sb_7Te_8)^{5+}$. The bond lengths within the $(Sb_3Te_4^+)_n$ cation fall into two groups. Sb–Te bonds within the $SbTe_6$ octahedra are long with 3.0257(5) and 3.0281(7) Å, and are in line with the corresponding bonds in the double-cube shaped $(Sb_7Te_8)^{5+}$ cluster in $Na(Sb_7Te_8)[GaCl_4]_6$ (3.012 Å).[4] The Te–Sb–Te angles at the central Sb(1) atom are close to the ideal values with distortions of less than 3°. The Sb–Te bond lengths at the peripheral 3-fold coordinated Sb(2) atoms are significantly shorter with 2.8685(9) Å. The bond angles at Sb(2) are, in turn, all close to rectangularity in the range between 87.18(1)° and 95.56(2)°.

A classical Lewis formula implies six covalent two-electron two-center bonds and a lone pair for the central Sb atom (Figure 2). With 14 valence electrons, this model is overstressed, and the bonding situation of this hypervalent Sb atom is better understood in nonclassical terms with three perpendicular three-center four-electron bonds.[4] The individual strands approach each other from the direction of the *a*-axis. Secondary Sb–Te bonds of 3.5375(8) Å connect the strands to an undulating layer parallel to the *a*–*b*-plane, which resembles a section of the 2D sheets, as present in the structure of Sb_2Te_3. The individual $(Sb_3Te_4^+)_n$ strand may be considered as a section of the layered structure of Sb_2Te_3 under formal loss of telluride ions: $Sb_2Te_3 = Sb_6Te_9 = Sb_6Te_8^{2+} + Te^{2-}$; $Sb_6Te_8^{2+} = Sb_3Te_4^+$. Alternatively, the structure of the cation may be understood as the product of a formal condensation of two $(Sb_2Te_2)^{2+}$ chains under the loss of one Sb^{3+} ion for each of the two Sb_2Te_2 groups according to $(Sb_2Te_2)^{2+} + (Sb_2Te_2)^{2+} = (Sb_3Te_4^+) + Sb^{3+}$. The structure motif of the $(Sb_3Te_4^+)_n$ chain is also present in the double-cube shaped discrete cation $(Sb_7Te_8)^{5+}$ with the typical 6-fold coordinated central Sb atom. These structural relations are summarized in Figure 3.

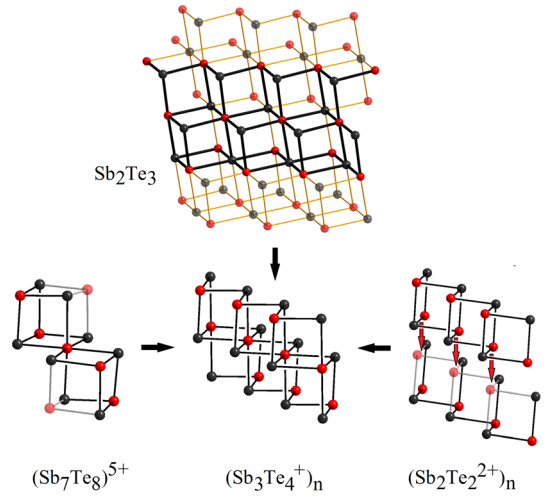

Figure 3. Structure of the 1D polymeric cation $(Sb_3Te_4^+)_n$ with the peculiar "double-ladder" structure as present in $(Sb_3Te_4)[GaCl_4]$ (**4**) and the structural relation to Sb_2Te_3 (top), $(Sb_7Te_8)^{5+}$ (bottom left), and $(Sb_2Te_2^{2+})_n$ (bottom right).

Statistical Disorder in the Anionic Part in the Structures of 2–4. The 1D-polymeric cations, as present in compounds **2**, **3a**, and **3b**, had already been found in the structures of $(Sb_2Te_2)Br[AlCl_4]$, $(Bi_2Te_2)Br[AlCl_4]$, and $(Bi_2Se_2)Br[AlCl_4]$.[14,15] The compounds in this study represent new combinations under exchange of chlorine for iodine in the case of **2**, and bromine and aluminum for chlorine and gallium for **3a** and **3b**. Despite coinciding formulas, the new structures are not isotypic to the reported ones, which crystallize in space group *C*2/*c*. Compounds **3a** and **3b** belong to space group *C*2/*m*. When the two cell axes are cut in half, the cell volume amounts to only one-quarter with respect to the reported congeners. Careful inspection of the diffraction patterns of several crystals did not show any superstructure reflections (Supporting Information Figure S3). The consequence is the necessity for a model of statistical disorder of the $[GaCl_4]^-$ groups. The atoms Ga and Cl(1) occupy their position in the mirror plane and close to the mirror plane by only 50%. Rows of tetrahedral $GaCl_4$ groups along the short *b*-axis emerge. The structure model implies order of the occupation of the Ga atoms in the *b*-direction, but no coherence between the rows, and a purely random occupation in the lattice directions *a* and *c* (Supporting Information Figure S4). An analogous disorder

DOI: 10.1021/ic502199v
Inorg. Chem. 2015, 54, 484–491

phenomenon is present in the structure of $(Sb_3Te_4)[GaCl_4]$ (**4**), which also belongs to space group $C2/m$. No evidence for an enlargement of the short unit cell axis b (4.1958(4) Å) by additional reflections was found on inspection of the diffraction pattern of several crystals (Supporting Information Figure S5). The structure can only be refined under the assumption of a disorder in the anionic part: a 50% occupation is assigned to the Ga and the Cl(1) atoms, giving a row of $[GaCl_4]^-$ groups along the b-axis. This structure model is only valid if there is no regularity between the occupation of the atom positions of the anions in the directions a and c (Supporting Information Figure S6).

In contrast, the diffraction patterns of $(Sb_2Te_2)I[AlI_4]$ (**2**) contain superstructure reflections. Taking these into account leads to a double b-axis and a primitive cell in space group $P2_1/n$ (Supporting Information Figure S7). The Fourier maps reveal a high electron density in the vicinity of Al(1). In the final refinement, two Al positions were assumed with a common occupation factor of unity as the sum of two individual ones. The respective positions gained the occupation factors 0.833(9) for Al(1) and 0.166(9) for Al(2). The disorder phenomena, as present in the structures of **3a**, **3b**, and **4** are partially, but not completely, resolved in the structure of **2** (Supporting Information Figure S8). In all crystal structures, the cationic part is not affected by any disorder. Since strong covalent bonds between pentele and chalcogen atoms are present in the directions of the respective strands, the cations determine the crystal lattice and afford different positions for the tetrahedral $[AlI_4]^-$ and $[GaCl_4]^-$ anions in the space between the strands. A similar disorder has been observed in the structure of $(Bi_4Te_4Br_2)(Al_2Cl_{6-x}Br_x)Cl_2$.[15]

Crystal Structure of 5: A Novel 1D-Polymeric $(SbTe_4^+)_n$ Cation. The structure of $(SbTe_4)[Ga_2Cl_7]$ consists of polymeric $(SbTe_4^+)_n$ cations and heptachloridodigallate anions. The $[Ga_2Cl_7]^-$ anions are of regular shape (Ga–Cl bonds 2.13(1)–2.33(1) Å, Cl–Ga–Cl angles 101.1(2)–116.9(2)°), and do not show remarkable deviations from those found in $K[Ga_2Cl_7]$.[30] The $(SbTe_4)^+$ cation is a five-membered ring in the envelope conformation. Within the ring, the bond lengths are rather equally distributed in the range 2.696(2)–2.832(2) Å, and the angles lie between 92.75(4)° and 103.09(4)°. The individual $(SbTe_4)^+$ rings are connected via Sb–Te bonds of 3.060(2) and 3.140(2) Å to a 1D polymer running along the crystallographic a-axis (Figure 4).

Each five-membered ring exhibits four heteronuclear bonds to two neighboring rings forming rectangular four-membered Sb_2Te_2 rings with inversion centers in the points of gravity as the links between the individual $(SbTe_4)^+$ cations. The two different intermolecular Sb–Te bonds generate a sequence of $(SbTe_4)^+$ clusters that are linked alternately by long and short bonds. This bond length alteration is a typical feature for clusters of the heavy main group elements and is attributed to the specific $5p^2 \rightarrow \sigma^*$ donor–acceptor bonds. If all bonds are assessed as two-center two-electron bonds, the Lewis formulas can be set up for the $(SbTe_4^+)_n$ cation, one of which is shown in Figure 4.

Only the Sb atom gains a hypervalency with four bonds, one lone pair, 10 valence electrons, and a negative formal charge. The Sb atom, however, may be positioned in all positions of the five-membered ring (Figure 5). All respective formulas reveal the charge +1 for the $SbTe_4$ cluster, and none of the five isomers can be excluded at the outset. Sb and Te atoms are difficult to distinguish from X-ray diffraction. The location of

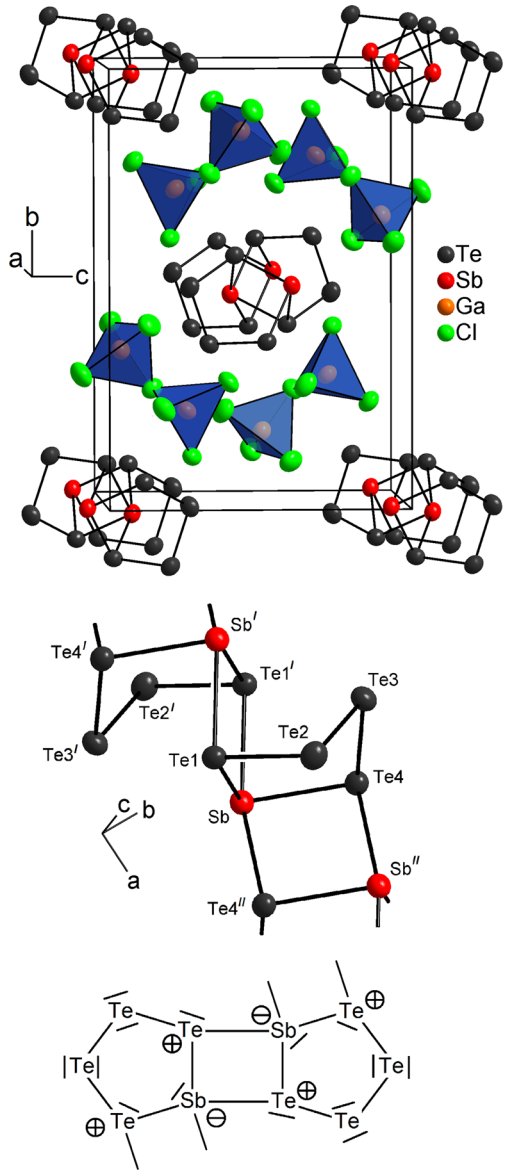

Figure 4. Unit cell of the structure of $(SbTe_4)[Ga_2Cl_7]$ (**5**) (top). The $[Ga_2Cl_7]^-$ ions are represented as discrete double tetrahedra. Atoms are drawn by thermal ellipsoids scaled to include a probability of 70%. In the middle, a detailed view of a section of the cationic chain is given; on bottom, the respective Lewis formula. Symmetry operations I: $-x$, $1-y$, $1-z$. II: $1-x$, $1-y$, $1-z$. Selected bond lengths/Å: Sb–Te1 2.833(2), Sb–Te1^{I} 3.060(2), Sb–Te4^{II} 3.140(2), Sb–Te4 2.817(2), Te2–Te3 2.696(2), Te3–Te4 2.774(2).

the Sb atom in the 4-fold coordinated position was, however, supported by the lowest occupation factor of all five crystallographic independent positions when refined as occupied by tellurium (see Experimental Section and Supporting Information Table S1).

In order to clarify the atom site distribution, all five conceivable isomers of the $(SbTe_4^+)_n$ cluster were calculated on a hybrid DFT level. As described in the Experimental Section, full optimization of the atomic positions was performed for each of the resulting unit cells. The results for relative stabilities of the five isomers, the Sb coordination number, and the next-neighbor Sb–Te distances are given in Table 3.

DOI: 10.1021/ic502199v
Inorg. Chem. 2015, 54, 484–491

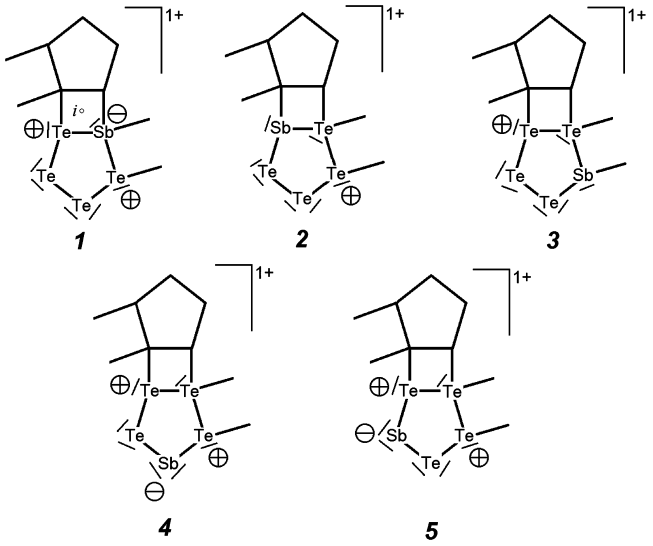

Figure 5. Lewis formulas of the five conceivable isomers of $(SbTe_4^+)_n$. By X-ray diffraction and by periodical DFT calculations, **1** was determined as the most reliable isomer with Sb in the position with the highest coordination.

Table 3. Relative Stability and Nearest-Neighbor Sb−Te Distances Calculated with PW1PW[a]

Sb at position	coordination number	relative energy/ kJ/mol	calcd nearest neighbor distances/Å
Sb	4	0	2.83, 2.84, 3.05, 3.15
Te1	3	+26	2.76, 2.88, 2.91
Te2	2	+84	2.73, 2.73
Te3	2	+105	2.39, 3.22
Te4	3	+34	2.76, 2.87, 2.87

[a]The numbering of the sites refers to Figure 4.

The energy minimum is clearly the isomer with Sb on the 4-fold coordinated position (isomer 1 in Figure 5). A direct correlation between the stability and the coordination number was found, with the 3-fold coordinated positions being 30 kJ/mol, and the 2-fold coordinated positions 80−100 kJ/mol even less stable. Even though zero-point, vibration, and entropy effects have been neglected, these differences are large enough that it is not expected that this would affect the conclusions. The calculated Sb−Te bond lengths range between 2.8 and 3.0 Å, similar to the distances obtained from the crystal structure determination. The exception is the isomer with Sb on the Te3 site where a very short (2.4 Å) and a rather long (3.2 Å) distance was obtained.

The analysis of the wave function based on a Mulliken population analysis led to an alternative explanation for the observed result. For all isomers, the atomic charge on Sb was very close to +1 while the Te atoms were almost neutral. Although atomic charges are not quantum-mechanical observables, and results from any population analysis should be regarded with care, this qualitative result is not expected to be method or basis set dependent. It explains why Sb prefers 4-fold coordinated sites since this is optimal for Sb^+ with four valence electrons. Since all Te atoms are neutral, they form two covalent bonds to their neighbor atoms, Te or Sb, and all other bonds are coordinative as in bulk Te.

CONCLUSION

Melts composed of $GaCl_3$ and AlI_3 are suitable and promising reaction media for the syntheses of compounds containing mixed, polymeric, chainlike polycations made up of pentele and chalcogen elements. Syntheses are performed by dissolving elemental Sb, Bi, Se, and Te in the presence of the respective pentele trihalide. Adjuvants have a crucial influence on the reactions and the product formation. Sodium or tetraphenylphosphonium halides were used. $[P(C_6H_5)_4]Cl$ and $GaCl_3$ achieve melts of low viscosity, which are liquid at room temperature. Six compounds with heteronuclear, cationic chains were synthesized and characterized by their chloridogallate and iodidoaluminate salts. The polymeric cations exhibit various structural motifs: $(Sb_2Te_2^+)_n$ is composed of approximately parallel arranged four-membered Sb_2Te_2 rings, $(Bi_2Ch_2^{2+})_n$ (Ch = Te, Se) and $(Sb_2Te_2^{2+})_n$ are ladder shaped strands, and $(Sb_3Te_4^+)_n$ represents a related double strand. The novel $(SbTe_4^+)_n$ cation consists of connected five-membered $SbTe_4$ rings in the envelope conformation.

ASSOCIATED CONTENT

Supporting Information

Crystallographic data in CIF format. Representations of the unit cells of **1** and **3a**; detailed tables of interatomic distances and angles in the crystal structures of **1**−**5**; elemental compositions of **1**−**5** obtained by EDX analyses; figures of the crystal structures of **1**, **3a**; simulated precession diagrams of zero and upper layers for **2**, **3a**, **3b**, **4**; figures explaining the anion disorder in the structures of **2**, **3a**, **4**; microscopic images of the crystals of **1**−**5**. This material is available free of charge via the Internet at http://pubs.acs.org.

AUTHOR INFORMATION

Corresponding Author

*E-mail: j.beck@uni-bonn.de.

Notes

The authors declare no competing financial interest.

ACKNOWLEDGMENTS

We thank Dr. Jörg Daniels, Christian Landvogt (University of Bonn), and Dr. Jonas Sundberg (University of Southern Denmark) for recording the single crystal diffraction data.

REFERENCES

(1) (a) Beck, J. *Coord. Chem. Rev.* **1997**, *163*, 55−70. (b) Brownridge, S.; Krossing, I.; Passmore, J.; Jenkins, H. D. B.; Roobottom, H. K. *Coord. Chem. Rev.* **2000**, *197*, 397−481. (c) Ahmed, E.; Ruck, M. *Coord. Chem. Rev.* **2011**, *255*, 2892−2903.

(2) Beck, J.; Schlüter, S.; Zotov, N. *Z. Anorg. Allg. Chem.* **2005**, *631*, 2450−2456.

(3) (a) Beck, J.; Schlüter, S.; Zotov, N. *Z. Anorg. Allg. Chem.* **2004**, *630*, 2512−2519. (b) Beck, J.; Dolg, M.; Schlüter, S. *Angew. Chem.* **2001**, *113*, 2347−2350.

(4) Eich, A.; Schlüter, S.; Schnakenburg, G.; Beck, J. *Z. Anorg. Allg. Chem.* **2013**, *639*, 375−383.

(5) Eich, A.; Hoffbauer, W.; Schnakenburg, G.; Bredow, T.; Daniels, J.; Beck, J. *Eur. J. Inorg. Chem.* **2014**, 3043−3052.

(6) Ahmed, E.; Isaeva, A.; Fiedler, A.; Haft, M.; Ruck, M. *Chem.—Eur. J.* **2011**, *17*, 6847−6852.

(7) (a) Zhang, Q.; Chung, I.; Jang, J. I.; Ketterson, J. B.; Kanatzidis, M. G. *J. Am. Chem. Soc.* **2009**, *131*, 9896−9897. (b) Ahmed, E.; Breternitz, J.; Groh, M. F.; Isaeva, A.; Ruck, M. *Eur. J. Inorg. Chem.* **2014**, 3037−3042.

DOI: 10.1021/ic502199v
Inorg. Chem. 2015, 54, 484−491

(8) (a) Beck, J. *Angew. Chem.* **1991**, *103*, 1149−1151. (b) Beck, J. *Z. Anorg. Allg. Chem.* **1993**, *619*, 237−242. (c) Beck, J.; Fischer, A.; Stankowski, A. *Z. Anorg. Allg. Chem.* **2002**, *628*, 2542−2548.
(9) Drake, G. W.; Schimek, G. L.; Kolis, J. W. *Inorg. Chem.* **1996**, *35*, 1740−1742.
(10) (a) Beck, J.; Stankowski, A. *Z. Naturforsch.* **2001**, *56 b*, 453−457. (b) Beck, J.; Fischer, A. *Z. Anorg. Allg. Chem.* **2002**, *628*, 369−372. (c) Feldmann, C.; Freudenmann, D. *Acta Crystallogr., Sect. C* **2012**, *68*, i68−i70.
(11) Baumann, A.; Beck, J. *Z. Anorg. Allg. Chem.* **2004**, *630*, 2078−2080.
(12) Beck, J.; Schlörb, T. *Phosphorus Sulfur Silicon Relat. Elem.* **1997**, *124* (125), 305−313.
(13) Beck, J.; Schlüter, S. *Z. Anorg. Allg. Chem.* **2005**, *631*, 569−574.
(14) Biswas, K.; Zhang, Q.; Chung, I.; Song, J.-H.; Androulakis, J.; Freeman, A. J.; Kanatzidis, M. G. *J. Am. Chem. Soc.* **2010**, *132*, 14760−14762.
(15) Biswas, K.; Chung, I.; Song, J.-H.; Malliakas, C. D.; Freeman, A. J.; Kanatzidis, M. G. *Inorg. Chem.* **2013**, *52*, 5657−5659.
(16) Kniep, R.; Mootz, D.; Rabenau, A. *Z. Anorg. Allg. Chem.* **1976**, *422*, 17−38.
(17) Beck, J.; Pell, M. A.; Richter, J.; Ibers, J. A. *Z. Anorg. Allg. Chem.* **1996**, *622*, 473−478.
(18) Sheldrick, G. M. *Acta Crystallogr.* **2008**, *A64*, 112−122.
(19) Otwinowski, Z.; Minor, W. *Methods in Enzymology*, Vol. 276, *Macromolecular Crystallography*, Part A; Carter, C. W., Jr., Sweet, R. M., Eds.; Academic Press: New York, 1997; pp. 307−326.
(20) *SADABS, Program for Absorption Correction from Area Detector Data*; Bruker AXS: Madison, Wisconsin.
(21) *DIAMOND, Program for Crystal Structure Visualisation*; Crystal Impact GbR: Bonn, Germany, 2005.
(22) Dovesi, R.; Orlando, R.; Erba, A.; Zicovich-Wilson, C. M.; Civalleri, B.; Casassa, S.; Maschio, L.; Ferrabone, M.; De La Pierre, M.; D'Arco, P.; Noel, Y.; Causa, M.; Rerat, M.; Kirtman, B. *Int. J. Quantum Chem.* **2014**, *114*, 1287−1317.
(23) Bredow, T.; Gerson, A. R. *Phys. Rev. B* **2000**, *61*, 5194−5201.
(24) Metz, B.; Stoll, H.; Dolg, M. *J. Chem. Phys.* **2000**, *113*, 2563−2571.
(25) Peterson, K. A.; Figgen, D.; Goll, E.; Stoll, H.; Dolg, M. *J. Chem. Phys.* **2003**, *119*, 11113.
(26) Dark red crystals of $Cu[AlI_4]$ were formed as a byproduct in reactions containing CuI and AlI_3. Lattice constants a = 11.8732(2) Å, c = 12.1086(4) Å, tetragonal space group $P\bar{4}2c$. The yellow rod shaped crystals turned out to be a new polymorph of $(SbI_2)[AlI_4]$ with lattice constants a = 10.8457(8) Å, b = 11.3104(9) Å, c = 10.8493(8) Å, β = 93.971(2)°, monoclinic space group $P2_1/n$. The yet unknown crystal structures will be subjected to forthcoming publications.
(27) (a) Voutsas, G. P.; Rentzeperis, P. J.; Siapkas, D. *Z. Kristallogr.* **1983**, *165*, 159−167. (b) Ibanez, A.; Jumas, J. C.; Olivier-Fourcade, J.; Philippot, E.; Maurin, M. J. *Solid State Chem.* **1983**, *48*, 272−283.
(28) Shevel'kov, A. V.; Dikarev, E. V.; Shpanchenko, R. V.; Popovkin, B. A. *J. Solid State Chem.* **1995**, *114*, 379−384.
(29) Voutsas, G. P.; Rentzeperis, P. J.; Siapkas, D. *Z. Kristallogr.* **1986**, *177*, 117−124.
(30) Mascheroa-Corral, P. D.; Vitse, P.; Potier, A. *Acta Crystallogr.* **1976**, *B32*, 247−250.

DOI: 10.1021/ic502199v
Inorg. Chem. 2015, 54, 484−491